

# LDA Analysis of Diesel Spray and Entrainment Air Flow

T.Obokata and T.Hashimoto

*Faculty of Engineering  
Gunma University  
1-5-1 Tenjin-cho  
Kiryu 376  
Japan*

H.Takahashi

*Gunma College of Technology*

## ABSTRACT

Transient velocities of fuel spray from a single hole injection nozzle of a Diesel engine and air movement around the spray are investigated under atmospheric conditions using a laser Doppler anemometer. The movement of the surrounding air is visualized using vectorial representation. It is found that the air is entrained after being pushed out by the spray and a large amount of air is entrained in the spray. The transient characteristics of the spray and the air flow, the profiles of the mean velocity, and the turbulence intensity and integral time scale of turbulence, are presented and compared with such values in the steady spray flow.

## INTRODUCTION

Many problems associated with the operation of the Diesel engine are yet to be solved. Among them are to raise their efficiency, to adapt them to varying fuels, and to minimize emission of pollutants. To solve such problems, it is necessary to study the combustion of a Diesel spray. From the injection of fuel to the exchange of gases in the cylinder, the stages of combustion related to heat and mass transfer must be analyzed. Since the air flow affects every stage of combustion significantly, it is absolutely necessary to measure the velocity of air flow and turbulence accurately.

With the advancement of the laser Doppler anemometer (LDA) technology in recent years it has become possible to measure the flow fields in internal combustion engines under firing condition. Swirl velocities in a fired Diesel engine have been measured (1). But its application to the Diesel spray in combustion is expected to be even more difficult (2). Therefore the authors have chosen to measure the velocity of an unconfined Diesel spray and the velocity of ambient gases entrained into the spray, as a first step of the study (3, 4).

Several research works have been carried out to analyze transient characteristics of Diesel spray, because of its importance in the investigation of Diesel combustion. However there are few reports on the direct measurement of the velocities within the spray (3, 4, 5), and the measurement of droplet size and velocity in

the spray (2, 6, 7).

The main objectives of the present experiment are to identify the flow fields of the Diesel spray and the ambient gases, and to obtain basic data needed for numerical simulation of the spray.

## EXPERIMENTAL PROCEDURE

### Fuel Injection System

Fig. 1 shows the experimental apparatus schematically. The fuel injection pump used was a Bosch A type (plunger diameter = 8mm). The nozzle was a single-hole type with a diameter of 0.31mm and a length of 0.6mm. The initial opening pressure of the valve ( $P_0$ ) was set at 9.8MPa. The two were connected with a pipe 600mm long having an inner diameter of 1.5mm. The fuel injection pump was driven by a motor at a frequency of 7.6Hz (457rpm). The entire injection system was fixed on a table that was movable in the horizontal direction.

The fuel injection was controlled by the rack of the pump. Its position (R) was read with a scale. The pressure inside the injection pipe was detected by a strain gauge pickup. The lift of the nozzle needle valve was measured with an eddy current gap sensor. Fig. 2 shows the variation of the nozzle needle valve's lift (l)

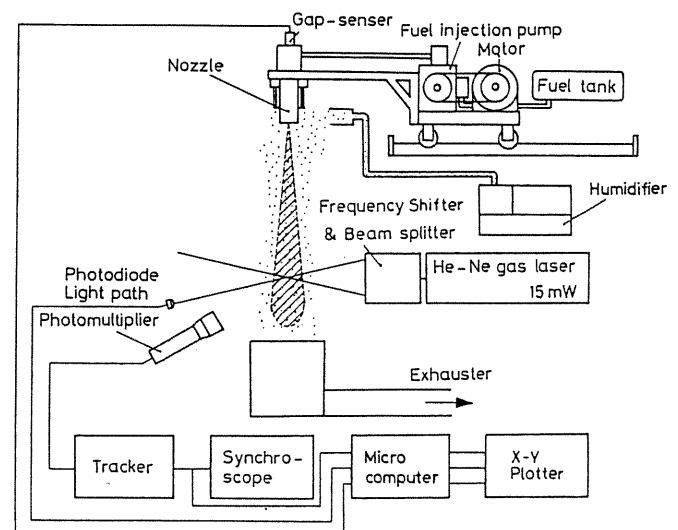


Fig. 1 Schematic of the system of experiment.

with the pressure ( $P$ ) inside the injection pipe on the nozzle side, at the rack position  $R = 6\text{mm}$ . It was found that the peak injection pressure was  $18.6\text{MPa}$ . Also an injection duration of about  $1.32\text{ms}$  was defined from the time difference between the half lift at the lift curve (1). The amount of injection per stroke ( $q$ ) was  $16.9\text{mm}^3$  in this experiment. The mean velocity of the fuel in the nozzle ( $\bar{V}_{0,c1}$ ) was estimated to be about  $169\text{m/s}$ . It was calculated from  $q$  divided by the cross-sectional area of nozzle and the duration of injection. JIS #2 Diesel oil was used as the fuel for this experiment.

Fig. 3 shows the spray tip penetration with time as indicated on the stroboscopic photographs of Fig. 4. The tip penetrates almost linearly at a velocity of  $110\text{m/s}$ .

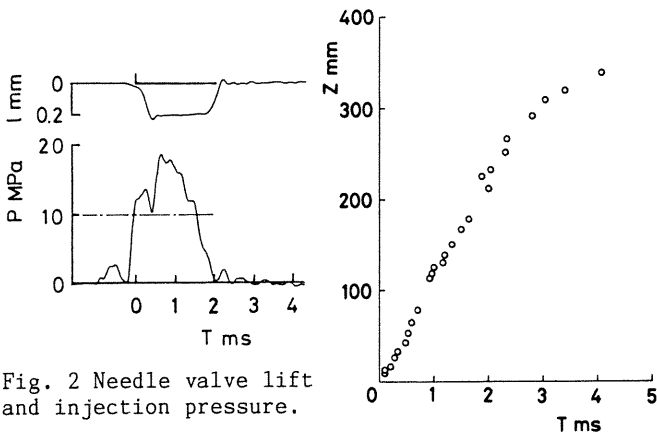


Fig. 2 Needle valve lift and injection pressure.

Fig. 3 Penetration of the spray.

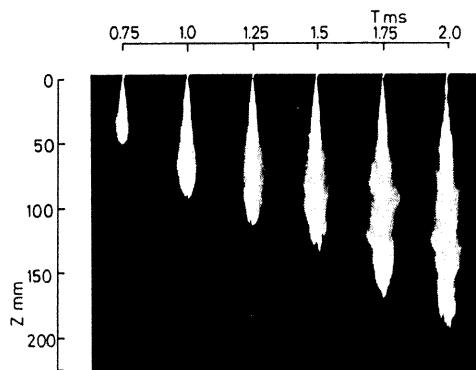


Fig. 4 Stroboscopic photographs of the spray.

#### Laser Doppler Anemometer (LDA)

The LDA optical system used was a DISA 55L Mark II. The total intersection angle of incidence of the laser beams was varied from  $16.24^\circ$  to  $2.18^\circ$  depending on the speed of the flow. When the angle of incidence was small and the volume was large (diameter  $0.5\text{mm}$  and overall length  $32\text{mm}$  at the angle of  $2.18^\circ$ ), observation was made at about  $30^\circ$  away from the forward direction and the effective length was decreased by about 10 times.

Scattering particles, (water droplets about  $6\mu\text{m}$  in average diameter) produced with an ultrasonic humidifier, were seeded in the ambient air flow. Also the velocities of fuel droplets were measured in the spray flow.

A tracker (DISA 55L37) was used as a signal processor. The velocity, pressure and lift

signals were recorded and processed with a microcomputer TEAC-PS9816 H5500 with a sampling frequency of  $85.3\text{kHz}$ .  $V$  and  $U$  denote the axial ( $Z$  direction) and radial ( $r$  direction) components of the flow velocities respectively.

#### Data Processing

Some examples of raw velocity output from the tracker are shown by dashed lines (axial velocity  $V$ ) in Fig. 5. The spray's flow measurement was taken with the operating point of the tracker initially shifted at around the expected spray velocity (3). Since the cycle to cycle variation is large in the flows inside and near the Diesel spray, the following data processing methods were used to analyze these transient flows.

Ensemble averaged analysis was used to obtain bulk flow velocities (mean velocity  $\bar{V}$  and  $\bar{U}$ ). Frequency discrimination method was also used to evaluate the turbulence intensity ( $v'$  rms and  $u'$  rms). In the latter method, bulk flow of each individual cycle ( $\bar{V}_c$  in Fig. 5) was estimated by lower frequency components less than cutoff frequency ( $f_c$ ) from the raw velocity ( $V$ ). The difference of  $V$  from  $\bar{V}_c$  refer to the cycle-resolved and instantaneous turbulence intensity (8).  $\bar{V}_m$  in Fig. 5 shows the bulk velocity obtained using a nonstationary time-averaged method (9). The differences between  $\bar{V}_c$  and  $\bar{V}_m$  are very small in these examples, because the cutoff frequency ( $f_c$ ) of  $667\text{Hz}$  corresponds to the moving window width ( $\Delta t$ ) of  $0.75\text{ms}$ .

The averaged bulk velocity ( $\bar{V}$ ), the turbulence intensity ( $v'$  rms) over 10 cycles, and the cyclic variation of bulk velocity ( $V'$  rms) are shown in Fig. 6. The fluctuation intensity ( $v'e$ ) at the ensemble averaged analysis is composed of the cyclic variation of bulk velocity ( $V'$  rms) and the turbulence intensity ( $v'$  rms) at the cycle-resolved analysis. The intensity of  $V'$  is often over the intensity of  $v'$  in this experiment.

The fast Fourier transform (FFT) analysis applied to the turbulence component of raw velocity at the stationary time window width ( $\Delta t$ ) was used to obtain the integral time scale of turbulence ( $L_t$ ), defined by the  $1/e$  point of the autocorrelation coefficient  $R(\tau)$  of the velocity. The effects of cutoff frequency or time window width on  $L_t$ ,  $\bar{V}$  and  $v'$  using this

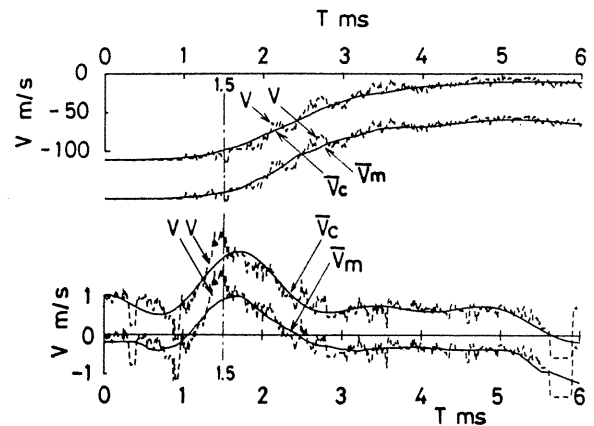


Fig. 5 Examples of raw velocity (dashed line) and bulk (mean) velocity (solid line).  
(a) Upper: Spray jet flow ( $Z=100\text{mm}$ ,  $r=0\text{mm}$ ).  
(b) Lower: Ambient air flow ( $Z=100\text{mm}$ ,  $r=20\text{mm}$ ).

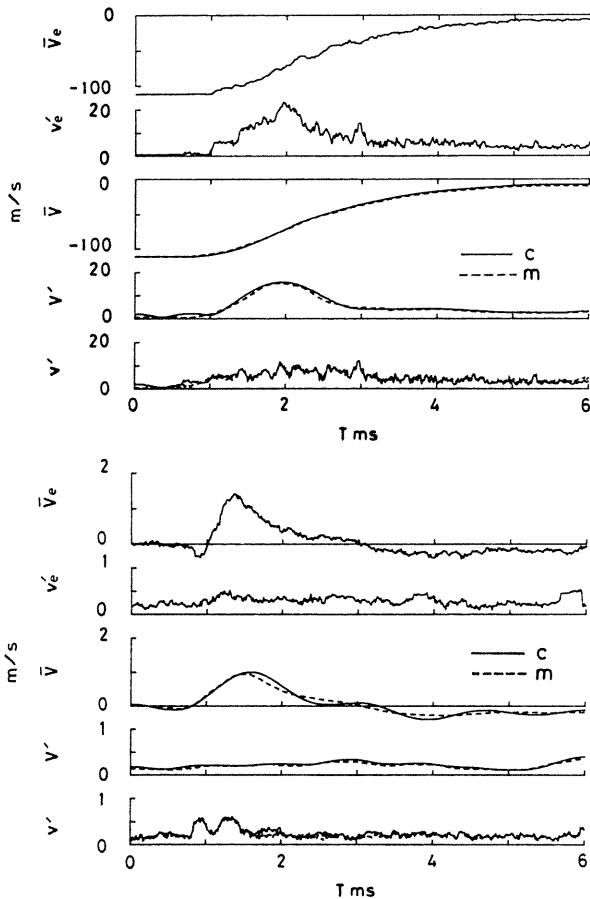


Fig. 6 Comparison of the data processing methods. ( $\Delta t = 0.75\text{ms}$ ,  $f_c = 667\text{Hz}$ ,  $f_s = 85.3\text{kHz}$ ). (a) Upper: Spray jet, (b) Lower: Ambient air flow

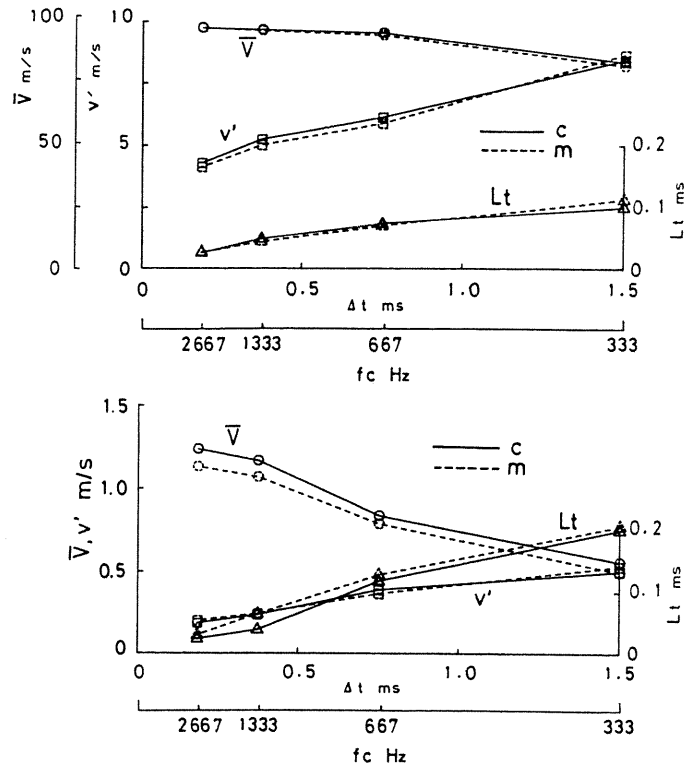


Fig. 7 Effects of sampling window width  $\Delta t$ . (The center of  $\Delta t$  is 1.5ms in Fig. 5) (a) Upper: Spray jet, (b) Lower: Ambient air flow

stationary time averaged analysis are shown in Fig. 7. In Fig. 5, a time  $T = 1.5\text{ms}$  after injection started corresponds to the center of each time window  $\Delta t$  at this analysis.  $\bar{V}$  and  $v'$  are the averaged values in the windows only for the cases shown in Fig. 7. The turbulence characteristics vary with the window's widths. But the differences in the averaging methods, frequency discrimination method (c, solid line) and nonstationary time-averaged method (m, dashed line), are little as shown in Fig. 6 and fig. 7.

In this experiment, the time window was set at  $0.75\text{ms}$  ( $f_c = 667\text{Hz}$ ) in the same way as the previous report (4). This corresponds to the crank angle width of 4.1 degrees of the four-stroke engine under a rotation speed of 914rpm (twice the frequency of injection). As illustrated in Fig. 8, transient spray and air flow are evaluated at 1.5 times of the arrival time of spray tip ( $T_a$ ) on the measuring point ( $Z_a$ ) in the penetration axis of the spray. Thus the first one third part of the spray flow represents the turbulence characteristics of these transient flows.

EXPERIMENTAL RESULTS

Spray Jet Velocity

Fig. 9 shows the time dependence of the radial (r) and axial (Z) distributions of axial velocity ( $\bar{V}$ ) of the spray. It is shown that the maximum radius of the spray is about 20mm and the highest velocity is about 110m/s at the tip and center of the spray at all times. The major part

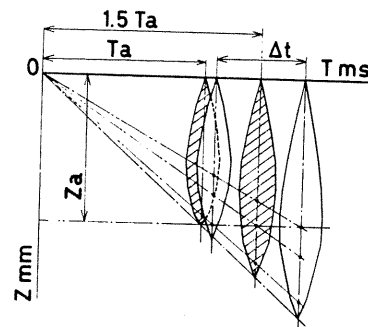


Fig. 8 The time and the part of spray represent the transient spray and air flow field

of the spray passes at  $T = 2\text{ms}$  at the measuring point of  $Z = 100\text{mm}$  (see also Fig. 4 and Fig. 5). But the velocity at the wake of the spray is less than 20m/s at 5ms and it decays rapidly.

Fig. 10 shows the axial (Z direction) distribution of the represented spray velocity ( $\bar{V}_{z,cl}$ ) divided by injection velocity ( $\bar{V}_{0,cl} = 169\text{m/s}$ ) along the center line of the spray. The dimensionless axial distance is obtained by using the diameter of the nozzle ( $d = 0.31\text{mm}$ ) and the density ratio of liquid fuel ( $\rho_l$ ) and ambient gas ( $\rho_g$ ). The shaded zone (measured) and the solid line (estimated) show that, the centerline velocity decay at a steady spray flow (10). Apart from the velocities near the nozzle (less than 75mm of Z), both the indicated velocities at  $1.5T_a$  and  $2.0T_a$  for all Z positions lie in the shaded zone. The Dimensionless half-radius ( $r_{0.5}/d$ ) of the spray's axial velocity at  $1.5T_a$  are plotted in Fig. 11. They take larger values than the shaded zone of

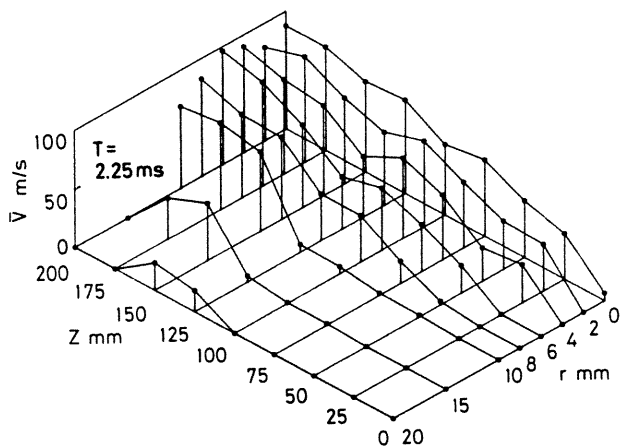
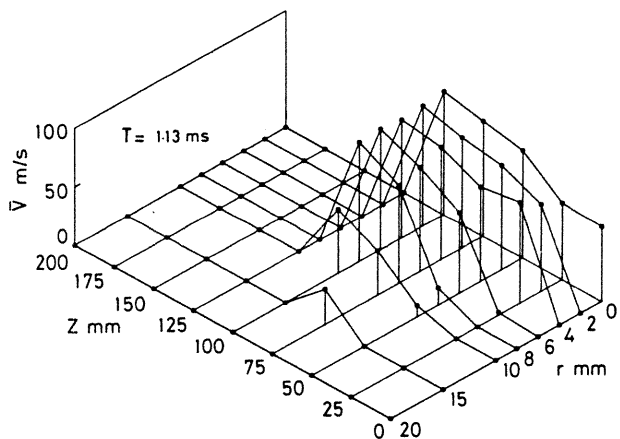


Fig. 9 Two dimensional distribution of axial spray velocity (ensemble averaged mean velocity).

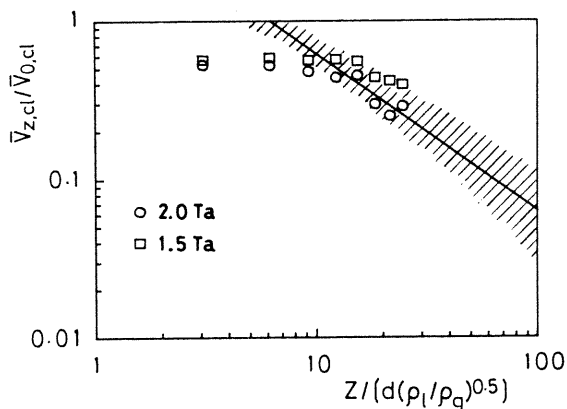


Fig. 10 Centerline velocity decay vs dimensionless axial distance.

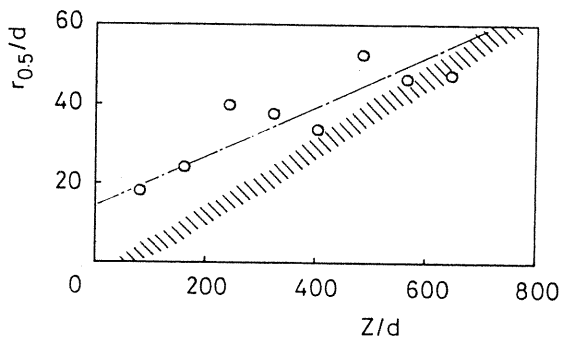
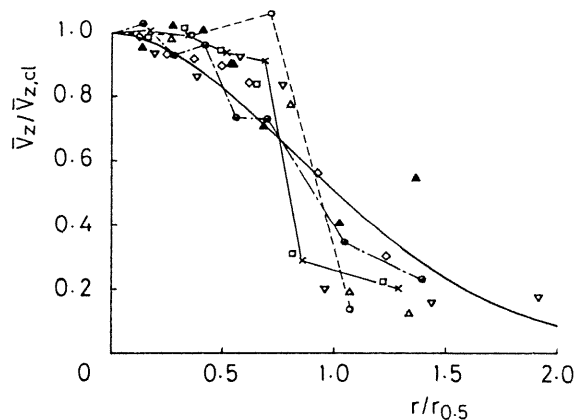
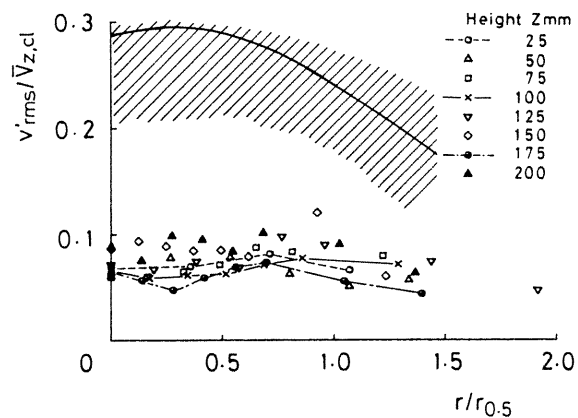


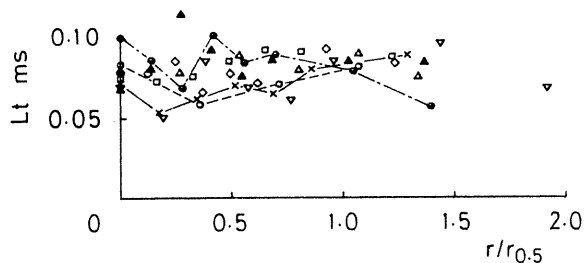
Fig. 11 Dimensionless half-radius of the axial velocity vs dimensionless axial distance.



(a) Dimensionless mean velocity.



(b) Dimensionless turbulence intensity.



(c) Integral time scale of turbulence.

Fig. 12 Turbulence characteristics of spray flow.

steady spray flow (10) at this transient spray flow.

Radial distribution of turbulence characteristics along the measuring height (Z direction) are shown in Fig. 12. The dimensionless expression is applied for axial velocity ( $\bar{V}_z$ ) and turbulence intensity ( $v'_{rms}$ ) divided by the velocity at  $r = 0$  in the same Z position ( $\bar{V}_{z,cl}$ ) at the time of  $1.5 Ta$ . The solid lines in Fig. 12 (a) and (b) indicate the values in the self-preserving jet (11) and the shaded zone denotes the data in the steady spray flow (10).

Mean velocity profiles near the nozzle take on larger values than the solid line at the inside of  $r/r_{0.5} = 0.8$ , and lower values at the outside. Then the profiles gradually close to the self-preserving jet along with the distances from the nozzle. Radial distribution of

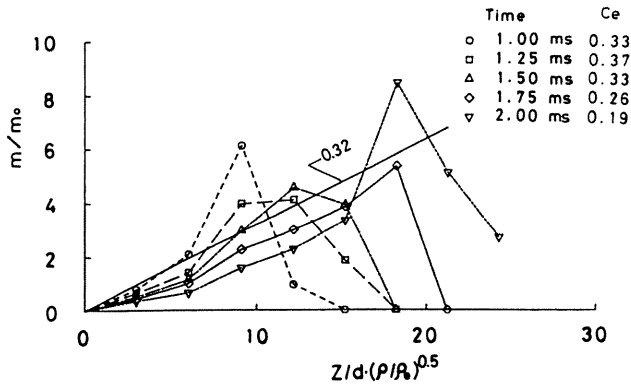


Fig. 13 Entrainment rate for spray jet.

turbulence intensity ( $v'$  rms) and integral time scale of turbulence ( $L_t$ ) are both flat and small because the frequency components lower than cutoff frequency (667Hz) are excluded in this transient spray flow. Averaged value of  $v'_{rms}/\bar{V}_{z,c1}$  is 0.08 and about one third of the steady spray flow. Mean value of  $L_t$  is about 0.08ms.

The changes of mass flow rate ( $m$ ) across a section at right angles to the spray axis ( $Z$ ) are plotted in Fig. 13. The  $m_o$  is the mass flow rate of fuel in the nozzle and  $\rho_o$  is density of fuel. The  $\rho$  is the density of air in substitution for the density of spray jet. The entrainment factor of  $C_e$  is represented by the formula.

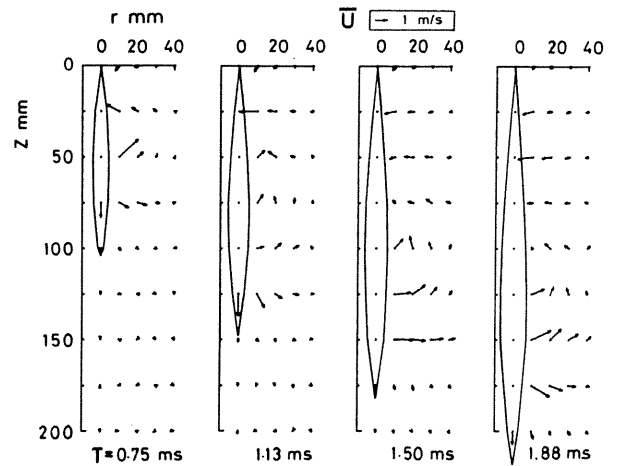
$$m/m_o = C_e \cdot (Z/d) \cdot (\rho / \rho_o)^{0.5} \quad (1)$$

$C_e$  takes a value of 0.32 in the steady axisymmetrical turbulent jet flow experiment (12). From the slope of the plotted data in Fig. 13,  $C_e$  were estimated at several instantaneous times and showed in the figure. The entrainment factor at this transient spray gives nearly the same value at steady jet flow; however  $m/m_o$  takes a larger value near the stagnation part of the spray.  $C_e$  decreased gradually after closing the needle valve.

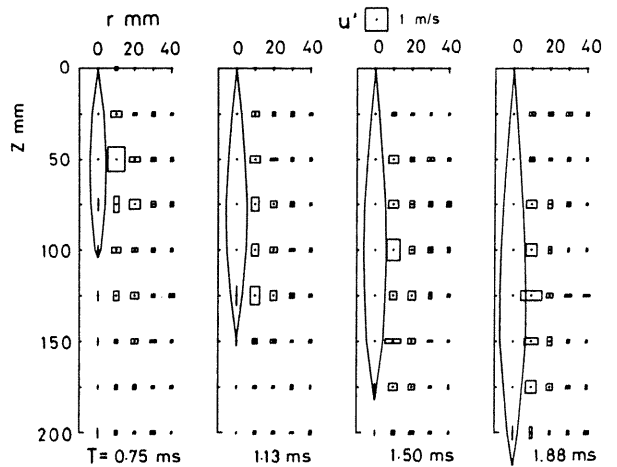
Velocity of the Air around the Spray

Fig. 14 (a) shows the time-related distribution of velocity vector obtained from the measured radial velocity  $U$  and axial velocity  $V$ . The air surrounding the spray is pushed outward. As the spray passes by the point of measurement, the velocity vectors rotate counterclockwise until they are opposite to the direction of advancement of the spray. As time passes, the vectors rotate more and the surrounding air entrains the spray. Until the spray passes by the point of measurement, the vectors rotate and become almost perpendicular to the axis of the spray. After the spray passes the point of measurement, it rotates counterclockwise and becomes parallel with the axis of spray. At larger values of  $r$  the phase of the vector rotation delays. This behavior is similar to that of a flow observed around a solid body moving in a quiescent fluid.

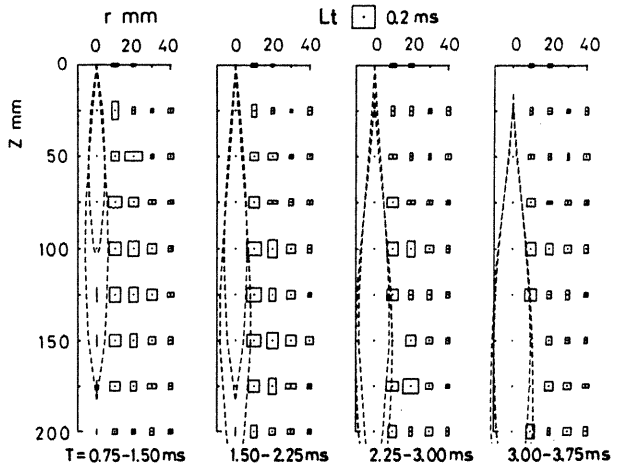
Turbulence intensity ( $u'$  rms,  $v'$  rms) and integral time scale of turbulence ( $L_t$ ) above the cutoff frequency (667Hz) are shown in Fig. 14 (b) and (c). Turbulence intensity distribution is the value at each instantaneous time shown below



(a) Mean velocity.



(b) Turbulence intensity.

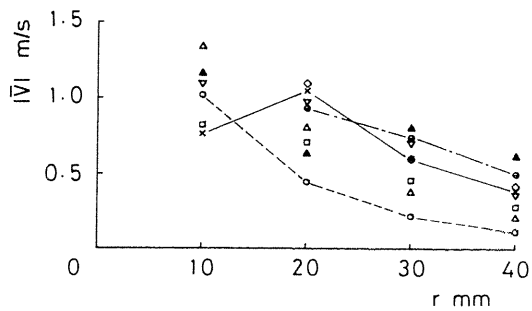


(c) Integral time scale of turbulence.

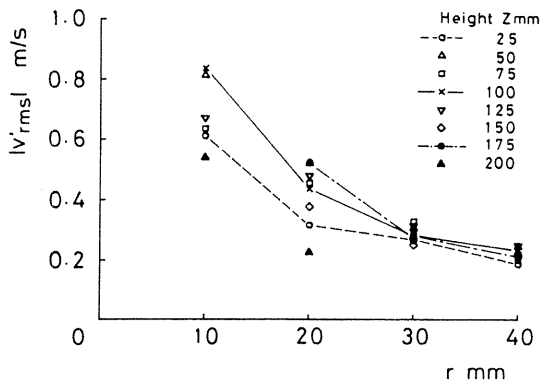
Fig. 14 Turbulence characteristics in the air flow around the spray.

the figure.  $L_t$  is given within the stationary time window width of 0.75ms. Both the intensity and the time scale of turbulence take on large values near the widest part of the spray.

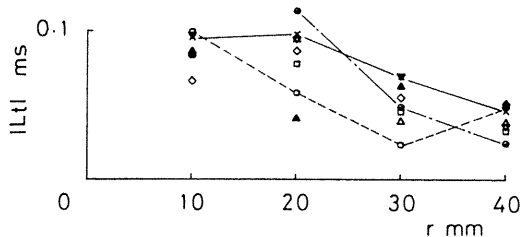
Turbulence characteristics of air flow around the spray at the representative time of spray (1.5Ta) on several measuring heights ( $Z$ ) are shown in Fig. 15. Each of the



(a) Mean velocity.



(b) Turbulence intensity.



(c) Integral time scale of turbulence.

Fig. 15 Radial distribution of turbulence characteristics along the axial distance.

characteristics here are absolute values consisting of two dimensional ( $r$  and  $Z$ ) components as illustrated in Fig. 14. Few measuring points covered by the spray are omitted from the figure. Depending on the measuring height, mean velocities near the spray is affected strongly by the spray. But all characteristics decay along the  $r$  direction. There are small differences in the respective characteristics along the  $Z$  direction. However smaller values are observed at the measuring height of 25mm.

The amount of air squeezed out and taken in by the spray through the cylindrical surface (200mm in height and 20mm in radius including the end surfaces) was estimated and showed in Fig. 16. The total amount of entrained air at  $T = 1.7\text{ms}$  is about 0.6ml which is 36 times the amount of injected liquid fuel per stroke.

## CONCLUSIONS

A Diesel fuel was sprayed into air at atmospheric conditions from a single-hole nozzle at a valve opening pressure of 9.8MPa, and the

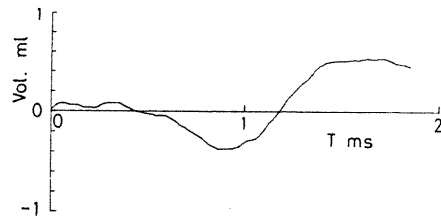


Fig. 16 Total amount of entrainment air

velocity of spray and surrounding air were measured by a laser Doppler anemometer (LDA). Transient characteristics of mean velocity ( $\bar{V}$ ), turbulence intensity ( $v'$  rms) and integral time scale of turbulence ( $L_t$ ) were presented.

The results of this experiment are summarized as follows:

1. Spatial distributions of mean velocity and turbulence characteristics of transient spray flow differ from the characteristics in steady spray flow.

2. The mean value of entrainment factor seems to be nearly the same for steady flow.

3. The flow around the spray is similar to that of a flow observed around a solid body moving in a quiescent fluid.

4. Spatial distributions of turbulence characteristics are measured in the flow around the spray.

This research was carried out under the financial support of RC-77 and RC-86 in JSME. The authors wish to express their appreciations to Diesel Kiki Co., Ltd. for offering the injection system used for this project. Thanks are also due to Mr. Waku and Mr. Sakurai who were then students in Gunma University for their cooperation.

## REFERENCES

1. Wigley, G., Patterson, A.C. and Renshaw, J., ASME Symposium on Fluid Mechanics of Combustion Systems, pp. 1-12, 1981.
2. Pitcher, G. and Wigley, G., Proc. Int. Conf. on Mech. of Two-Phase Flows, pp. 291-298, 1989.
3. Obokata, T., Inaba, K. and Takahashi, H., Proc. 4th. Int. Symp. on Appl. of Laser Anemometry to Fluid Mech., Paper No. 3.15, 1988.
4. Hashimoto, T., Obokata, T., Waku, T. and Takahashi, H., Trans. of SAEJ., No. 45, (in press), 1990, (in Japanese).
5. Chehroudi, B. and Bracco, F.V., SAE Paper No. 880522, 1988.
6. Maeda, M., Hishida, K., Sekine, M. and Watanabe, N., Proc. 3rd Int. Symp. on Appl. L. A. to F. Mech., Paper No. 20.3, 1986.
7. Arcoumanis, C., Cossali, E., Paal, G. and Whitelaw, J.H., SAE Paper No. 890314, 1989.
8. Fansler, T.D. and French, D.T., SAE Paper No. 880377, 1988.
9. Lancaster, D.R., SAE Paper No. 760159, 1976.
10. Wu, K.-J., Santavicca, D.A., Bracco, F.V. and Coghe, A., AIAA Journal, Vol. 22, pp. 1263-1270, 1984.
11. Wygnanski, I. and Fiedler, H., J.F.M., Vol. 38, pp. 577-612, 1969.
12. Ricou, F.P. and Spalding, D.B., J.F.M., Vol. 11, pp. 21-32, 1961.